EBioMedicine 17 (2017) 45–56

Contents lists available at ScienceDirect

EBioMedicine

journal homepage: www.ebiomedicine.com

Research Paper

Cancer-associated Fibroblasts Promote Irradiated Cancer Cell Recovery Through Autophagy

Yongbin Wang [a,1], Guifang Gan [a,1], Bocheng Wang [b], Jinliang Wu [b], Yuan Cao [a], Dan Zhu [b], Yan Xu [a], Xiaona Wang [a], Hongxiu Han [b], Xiaoling Li [c], Ming Ye [d,*], Jiangmin Zhao [b,*], Jun Mi [a,*]

[a] Department of Biochemistry & Molecular Cell Biology, Key Laboratory of Cell Differentiation and Apoptosis of Chinese Ministry of Education, Shanghai Jiao Tong University School of Medicine, China
[b] 9th Affiliated Hospital of Shanghai Jiao Tong University School of Medicine, China
[c] NIEHS, National Institute of Health, United States
[d] Renji Hospital, Shanghai Jiao Tong University School of Medicine, China

ARTICLE INFO

Article history:
Received 12 January 2017
Received in revised form 17 February 2017
Accepted 20 February 2017
Available online 22 February 2017

Keywords:
Cancer-associated fibroblast
Cytokines
Intermediate metabolite
Autophagy
Tumor relapse
Radiation therapy

ABSTRACT

Tumor relapse after radiotherapy is a significant challenge to oncologists, even after recent the advances in technologies. Here, we showed that cancer-associated fibroblasts (CAFs), a major component of cancer stromal cells, promoted irradiated cancer cell recovery and tumor relapse after radiotherapy. We provided evidence that CAFs-produced IGF1/2, CXCL12 and β-hydroxybutyrate were capable of inducing autophagy in cancer cells post-radiation and promoting cancer cell recovery from radiation-induced damage *in vitro* and *in vivo* in mice. These CAF-derived molecules increased the level of reactive oxygen species (ROS) post-radiation, which enhanced PP2A activity, repressing mTOR activation and increasing autophagy in cancer cells. Consistently, the IGF2 neutralizing antibody and the autophagy inhibitor 3-MA reduce the CAF-promoted tumor relapse in mice after radiotherapy. Taken together, our findings demonstrated that CAFs promoted irradiated cancer cell recovery and tumor regrowth post-radiation, suggesting that targeting the autophagy pathway in tumor cells may be a promising therapeutic strategy for radiotherapy sensitization.

1. Introduction

The initiation and progression of tumors are controlled not only by tumor cells but also by their surrounding stromal cells (Lengauer et al., 1998; Ronnov-Jessen et al., 1996; Tlsty, 2001; Carmeliet and Jain, 2000; Sandler et al., 2004). Cancer-associated fibroblasts (CAFs), are major components of cancer stromal cells that account for about 40%–50% of the total cell population in cancers (Xing et al., 2015). CAFs are primarily derived from activated quiescent fibroblasts surrounding the cancer cells, and have been shown to directly promote tumor initiation (Bhowmick et al., 2004; Olumi et al., 1999), progression (Dimanche-Boitrel et al., 1994; Orimo et al., 2005), and metastasis (Grum-Schwensen et al., 2005; Olaso et al., 1997). CAFs produce extracellular matrix-degrading enzymes, secrete growth factors and cytokines, and export a large amount of metabolites, which collectively promote tumor development and progression (Kolch et al., 1995; Saharinen et al., 2011; Boire et al., 2005; Lochter et al., 1997; Chaudhury et al., 2010; Ding et al., 2010) (Bonuccelli et al., 2010; Capparelli et al., 2012; Fiaschi et al., 2012).

Tumor relapse after radiotherapy is a significant challenge to oncologists. Tumor recurrence was generally due to radiation resistance, which was determined by both the intrinsic characteristics and the extrinsic microenvironment of cancer cells (Frank et al., 2010). The unique stem cell properties, including dormancy state (Bao et al., 2013) and enhanced DNA damage repair capacity (Bao et al., 2006), increased the resistance of cancer cells to radiation (Visvader and Lindeman, 2008). The particular niche in tumor tissues also enhanced tumor resistance to radiation (Yang and Wechsler-Reya, 2007). The *in vitro* study has demonstrated that pretreatment with CAF-conditioned medium promoted HeLa cell survival post-radiation (Chu et al., 2014). Further studies demonstrated that preexisting CAFs promoted cancer cell resistance to radiation through the paracrine pathway of insulin-like growth factor (IGF)1/2 (Chen et al., 2014). The IGF1 receptor signaling, in turn, induced tumor stem-like cell formation and increased radiation resistance of immortalized Igf2 null mouse embryonic fibroblasts and glioma stem cells (Burns and Hassan, 2001; Osuka et al., 2013). All these

Abbreviations: CAFs, cancer-associated fibroblasts; IGF1/2, insulin-like growth factor 1/2; CXCL12, C-X-C motif chemokine ligand 12; ROS, reactive oxygen species; PP2A, serine/threonine protein phosphatase 2A; mTOR, mechanistic target of rapamycin; 3-MA, 3-methyladenine.

* Corresponding authors.
E-mail addresses: yeming@renji.com (M. Ye), johnmzhao@sjtu.edu.cn (J. Zhao), jmei@sjtu.edu.cn (J. Mi).

[1] These authors contribute equally to this study.

http://dx.doi.org/10.1016/j.ebiom.2017.02.019

observations suggested that preexisting CAFs enhanced radiation resistance of tumor cells before radiation therapy. However, it is not clear whether CAFs play roles in irradiated cancer cell recovery.

In this study, we found that CAFs promoted irradiated cancer cell recovery and promoted tumor relapse after radiation therapy, which was further confirmed by the enhancement of IGF2 neutralizaing antibody on radiotherapy results. Moreover, our study demonstrated that CAFs promoted cancer cell recovery through inducing cancer cell autophagy post-radiation and the autophagy inhibitor 3-methyladenine (3-MA) enhanced the efficacy of radiotherapy, suggesting that CAFs are critical factors for tumor recurrence after radiotherapy. Therefore, targeting the autophagy pathway may be a promising therapeutic strategy for radiotherapy sensitization, and we hypothesize that autophagy inhibitors will improve radiotherapy efficacy.

2. Materials & Methods

2.1. Cell Culture and Reagents

Lung cancer A549 and melanoma A375 cells (ATCC, Manassas, VA) were cultured in DMEM with 10% FBS. Glucose-deprived DMEM was purchased from Gibco (Grand Island, NY). Human recombinant TGF-β1, IGF1, IGF2, CSCL12, EGF, was purchased from Peprotech (Suzhou, China). SYBR Green PCR master mix and the TaqMan microRNA reverse transcription kit were purchased from ABI (Foster City, CA). The source for antibodies used for immunoblotting (IB) were as follows: Akt, phospho-AKT (T308), phospho-GSK-3β, S6K, phospho-S6K, mTOR, phospho-mTOR, ERK, phospho-ERK, β-catenin (Cell Signaling Technology, MA, USA), GSK-3β (Epitomics, CA, USA), PP2A (ABclonal, ProteinTech), and β-actin (Santa Cruz Biotechnology, CA, USA). The neutralization antibodies against IGF1, IGF2 and CXCL12 were purchased from the R & D. 3-MA was purchased from the Selleck.

2.2. Isolation and Identification of Cancer-associated Fibroblast

Human normal primary fibroblasts and cancer-associated fibroblasts were isolated from foreskin or from lung cancer tissues, respectively. After posthectomy, the foreskins were immediately transported to the laboratory on ice. The foreskins were minced and then digested with 0.1% type I collagenase and trypsin. After digestion, the tissue was filtered with a 400-mesh sieve, and the filtrate was centrifuged at 1000 ×*g* for 10 min. Cells obtained from the pellet were cultured with DMEM containing 10% FBS for 2 h; the attached cells, verified by F-actin staining (Fig. 1), were fibroblasts. After 3 passages, the cells were frozen in liquid nitrogen for further experiments.

2.3. Cellular ROS (Reactive Oxygen Species) Evaluation

The 2,7-dichlorodihydrofluorescein diacetate (DCFH-DA, Sigma) was used as a cellular ROS indicator. The DCFH-DA was transformed into 2,7-dichlorodihydrofluorescein (DCFH) by the esterases, which could be further oxidized to a highly fluorescent compound 2,7-dichlorofluorescein (DCF) by ROS. Cells were co-cultured with the 10 μM of DCFH-DA for 20 min, and analyzed by flow cytometry. The intensity of DCF represented intracellular ROS levels.

2.4. Lentiviruses-mediated Stable Cell Lines

Short-hairpin sequences targeting IGF1 (NM_001111283.2), IGF2 (NM_000612.5), and CXCL12 (NM_000609.6), ATG5 (NM_001111283.2) was synthesized (Sangon Biotech) and separately inserted into the pGIPZ lentiviral vector (Open Biosystems, Lafayette, CO). These lentiviral plasmids were co-transfected into 293T cells with psPAX2 and pMD2G to generate the lentiviruses using Lipofectamine 2000 (Invitrogen, CA). Viruses were collected from the supernatant of transfected 293T cells 3 days after transfection. The specific shRNA sequences were as following: IGF1-SH1: sense: 5′-CCGGCCCGTCCCTATCGACAAACAACTCGAGTTGTTTGTCGATAGGGACGGGTTTTTG-3′; antisense: 5′-AATTCAAAAACCCGTCCCTATCGACAAACAACTCGAGCCCGTCCCTATCGACAAACAA-3′. IGF1-SH2: sense: 5′-CCGGGCTTCTCACCTTCTTGGCCTTCTCGAGAAGGCCAAGAAGGTGAGAAGCTTTTTG-3′; antisense: 5′-AATTCAAAAAGCTTCTCACCTTCTTGGCCTTCTCGAGAAGGCCAAGAAGGTGAGA-AGC-3′. IGF1-SH3: sense: 5′-CCGGCCAATATGACACCTGGAAGCACTCGAGTGCTTCCAGGTGTCATATTGGTTTTTG-3′; antisense: 5′-AATTCAAAAACCAATATGACACCTGGAAGCACTCGAGTGCTTCCAGGTGTCA-TATTGG-3′. IGF1-SH4: sense: 5′-CCGGCTCGTGCTGCATTGCTGCTTACTCGAGTAAGCAGCAATGCAGCACGAGTTTTTG-3′; antisense: 5′-AATTCAAAAACTCGTGCTGCATTGCTGCTTACTCGAGTAAGCAGCAAT-GCAGCACGAG-3′. IGF2-SH1: sense: 5′-CCGGGCATCGTTGAGGAGTGCTGTTCTCGAGAACAGCACTCCTCAACGATGCTTTTTG-3′; antisense: 5′-AATTCAAAAAGCATCGTTGAGGAGTGCTGTTCTCGAGAACAGCACTCCTCAACGATGC-3′. IGF2-SH2: sense: 5′-CCGGGAGTGCAGGAAACAAGAACTACTCGAGTAGTTCTTGTTTCCTGCACTCTTTTTG-3′; antisense: 5′-AATTCAAAAAGAGTGCAGGAAACAAGAACTACTCGAGTAGTTCTTGTTTCCTGCACTCC-3′. IGF2-SH3: sense: 5′-CCGGCCTCCCAAATTGCTGGGATTACTCGAGTAATCCCAGCAATTTGGGAGGTTTTTG-3′; antisense: 5′-AATTCAAAAACCTCCCAAATTGCTGGGATTACTCGAGTAATCCCAGCAATTTGGGAGGC-3′. CXCL12-SH1: sense: 5′-CCGGCAAACTGTGCCCTTCAGATTGCTCGAGCAATCTGAAGGGCACAGTTTG-TTTTTG-3′; antisense: 5′-AATTCAAAAACAAACTGTGCCCTTCAGATTGCTCGAGCAATCTGAAGGGCACAGTTTG-3′. CXCL12-SH2: sense: 5′-CCGGCCGTCAGCCTGAGCTACAGATCTCGAGATCTGTAGCTCAGGCT-GACGGTTTTTG -3′; antisense: 5′-AATTCAAAAACCGTCAGCCTGAGCTACAGATCTCGAGCCGTCAGCCTGAGCTACAGAT -3′. ATG5-SH1: sense: 5′-CCGGGCACCCATCTTTCCTTAACGAAACTCGAGTTTCGTTAAGGAAAGATGGGTTTTTTTG -3′; antisense: 5′-AATTCAAAAACACCCATCTTTCCTTAACGAAACTCGAGTTTCGTTAAGGAAAGATGGGTT-3′. ATG5-SH4: sense: 5′-CCGGGCATGAAAGAAGCTGATGCTTTACTCGAGTAAAGCATCAGCTTCTTTCATATTTTTG-3′; antisense: 5′-AATTCAAAAACATGAAAGAAGCTGATGCTTTACTCGAGTAAAGCATCAGCTTCT-TTCATA-3′.

2.5. Immunoprecipitation and Western Blotting

The cells were placed on ice and washed with ice-cold PBS. Total protein extract was prepared with the appropriate amount of RIPA lysis buffer (25 mM tris-HCl at pH 7.5, 2 mM EDTA, 25 mM NaF and 1% Triton X-100) containing 1 × protease inhibitor mixture (Roche Inc., CH, Switzerland) and 1 × PMSF.

The proteins were resolved on 7–15% SDS-polyacrylamide gels and transferred by electroblotting to nitrocellulose membranes (Bio-Rad Inc., CA, USA). The membranes were blocked with 5% nonfat dry milk in TBST (the mixture of tris-buffered saline and Tween 20) for 1 h. Proteins of interest were detected with specific antibodies, blots were scanned using an Odyssey infrared imaging system (LI-COR), and proteins were quantitatively analyzed using the Odyssey software.

2.6. Cytokine Array

The CAFs or fibroblasts were cultured in serum-free medium when they grew to 90% confluence. Growing for another four days, the media were collected and concentrated, and followed by dialysis. After labeling with biotin, samples were incubated with the antibody array chip (AAH-B LG-1, Raybiotech) for 2 h. Then, chips were reacted with streptavidin-conjugated fluorescene dye, and detected by the Axon Genepix scanner The data were normalized to the total protein.

2.7. Patients and Eligibility

This study was approved by the Ethical Review Board of the Medical Faculty of the Shanghai Jiao-Tong University School of Medicine.

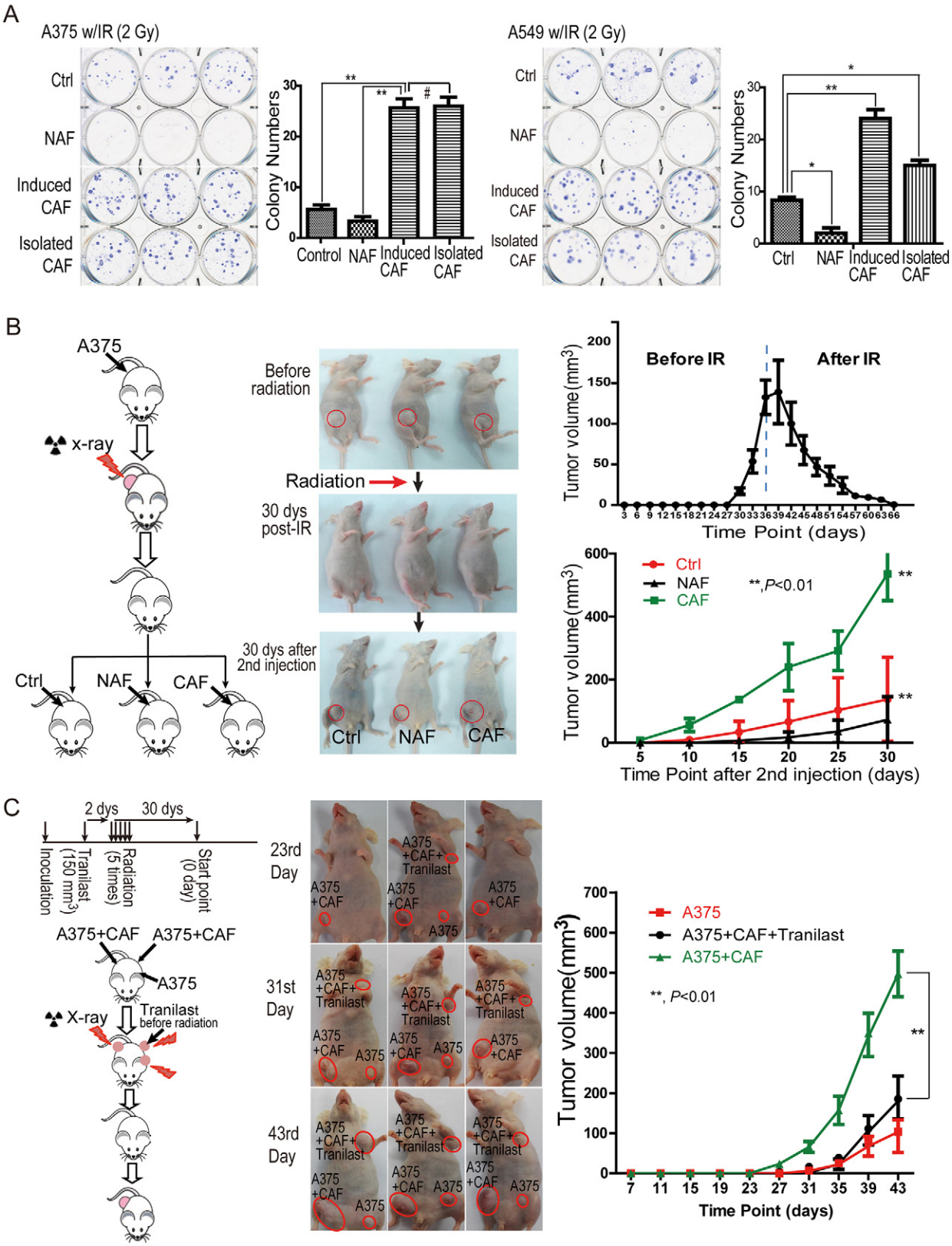

Fig. 1. CAFs promoted irradiated cancer cell recovery *in vitro* and tumor recurrence post-radiation in a mouse model. A. CAFs contribute to melanoma A375 cell and lung cancer A549 cell recovery from radiation-induced cell death *in vitro*. A375 or A549 cells were cultured in CAF- or primary fibroblast-conditioned medium immediately radiation treatment. *, $p < 0.01$; #, $p > 0.05$. The colonies were counted and visualized 2 weeks after radiation (mean ± SD). B. CAFs promoted melanoma relapse in the xenografted mice (model 1). The mice were treated as shown in the schematic. CAFs were injected into existing tumor sites 30 days after radiation. Tumor volumes are presented as mean ± SD. C. CAFs promoted melanoma relapse in the xenografted mice (model 2). The experiment was performed as shown in the schematic drawing. The tumors whose volumes had reached 150 mm^3 were locally injected with 100 μL Tranilast (200 μM) daily for 1 week, followed by a total of 30 Gy radiation in five fractions of 6 Gy each. The tumor volumes are presented as mean ± SD.

Ninety-six primary lung cancer patients, who were histologically confirmed at stage I/II, and 44 primary liver cancer patients, who were diagnosed and histologically confirmed at stage I, were eligible for this study, and all patients had not received surgery. Patients from ages 48–87 years were treated at the Shanghai Renji Hospital, Shanghai 3rd People's Hospital or Shanghai Ruijin Hospital since 2008. These eligible patients received either EBRT or SBRT, for a total dose of radiation at 65 ± 5 Gy. The follow-up investigations were executed every month, and the primary end point was patient death.

2.8. Clonogenic Assays

The clonogenic assay was adapted from Franken et al. (2006). Briefly, cells were treated or untreated with radiation at 6 h after re-seeding in a 100 mm dish at a density of 400 cells per dish. Conditioned medium at a ratio of 1:3 or cytokines/chemokines at the indicated concentrations were added into the culture medium immediately radiation. After approximately 14 days of incubation, the cells were fixed and stained with crystal violet, and colonies containing at least 50 cells were scored.

2.9. Multi-voxel ^{1}H Magnetic Resonance Scanning Analysis and MRI Image

Patients were first positioned for the parallel and sagittal T2W1 MRI scanning (1.5 T MRI scanner, GE Signa) with fat suppression. The parameters for MRI were as follows: the TE was 108 ms, the TR was 5000 ms, the thickness was 5 mm, the layer spacing was 0 mm, the FOV was 24 cm, the matrix was 320 × 224, and the NEX was equal to 2. Then, based on the position of the tumor, the SI-PRESS sequence (TR 1000 ms, TE 35 ms, NEX = 1) was executed in the study with a voxel size of 18 mm^3. Eventually, the peak value of 3.2 ppm and 1.3 ppm in the MRS data were analyzed by the SER software in the function tool.

2.10. Xenografted Mouse Model

Four-week-old BALB/c nude mice were obtained from the Shanghai SLAC Laboratory Animal Center (Shanghai, China). The animals were handled according to the protocol approved by the Institutional Animal Care and Use Committee of the Shanghai Jiao Tong University School of Medicine. Tumor xenografts were generated by subcutaneous inoculation of A375/A549 cells or by co-injecting human fibroblasts with A375/A549 cells (the ratio of fibroblasts to A375 cells was 3:1, and the cancer cell number in each injection was 1×10^6 cells) bilaterally into the armpits. There were 10 tumors at each group. Both non-activated fibroblasts (NAF) and CAFs were treated with radiation before injection at the dose of 6 Gy, a half lethal dose to fibroblast. The tumor volume was determined at the indicated time points using digital caliper measurements and the following formula: tumor volume (mm^3) = ½ × longest diameter^2 × shortest diameter. At the indicated time points, the mice were sacrificed and the tumors were excised.

2.11. Comet Assay

The comet assay was performed under neutral conditions according to the procedure of Singh et al. (1988) with modifications by Klaude et al. (1996). The A549 cells treated with CAF-conditioned medium, control medium, or IGF2 were irradiated at doses of 2 Gy. After radiation the cells were allowed to repair for 30, 60, 180, and 360 min, or harvested immediately (time 0 = no repair) and were suspended in 1.0% low-melting agarose dissolved in PBS and layered onto microscope slides previously covered with 0.5% normal melting point agarose. Cells were lysed at 37 °C overnight in a buffer consisting of 2% sarkosyl, 500 mM EDTA, 0.5 mg/mL protein K, pH 8.0. Next, the DNA was unwound and uncoiled in electrophoresis buffer containing of 90 mM boric acid, 90 mM tris Cl and 2 mM EDTA (pH 8.5) for 30 min. Then electrophoresis was carried out in the dark and the cells were stained with 4′,6-diamidino-2-phenylindole (DAPI) solution. The slides were examined with an Eclipse fluorescence microscope (Nikon, Tokyo, Japan). The comet tail moment was measured in one hundred cells randomly selected from each sample. Each experiment was repeated three times.

2.12. Analysis of PP2A Activity

To analyze the effect of IGF2 on phosphatase activity of PP2A post-radiation, the phosphorylation of PP2Ac at T307 was analyzed in A549 cells or 293T cells overexpressing wild type or mutant PP2Ac (1 Gy). The PP2A phosphatase activity was indicated by the T307 dephosphorylation of PP2Ac.

2.13. Statistical Analysis

The animal data are presented as the medians ± SD, whereas other data are presented as the means ± SD. All data are representative of at least three independent experiments. The differences between groups were assessed by a Student's *t*-test. All reported differences are $p < 0.05$ unless otherwise stated.

3. Results

3.1. CAFs Promoted Irradiated Cancer Cell Recovery In Vitro and Tumor Recurrence Post-radiotherapy in a Mouse Model

To determine whether CAFs are capable of promoting irradiated cancer cell recovery, radiation-treated melanoma A375 cells were immediately cultured in CAF- or fibroblast-conditioned medium. The radiation-treated A375 cells without conditioned medium were used as controls. As shown in Fig. 1A, significantly more A375 cells survived after radiation when cultured in conditioned medium from either isolated CAFs or induced CAFs. The number of colonies originating from the cells that survived increased from 4 or 5 to 24 (per dish) compared to the control or the fibroblast-conditioned medium group (Fig. 1A). Similar results were obtained from lung cancer A549 cells, indicating that CAFs promoted cancer cell recovery from radiation-induced damage.

To further investigate whether CAF-mediated irradiated cancer cell recovery enhanced cancer recurrence *in vivo*, we injected melanoma A375 cells into abdominal armpits of nude mice, followed by a total of 30 Gy radiation in five fractions of 6 Gy once the volume of tumors reached 150 mm^3 (Fig. 1B). When the tumors were undetectable by visual check after radiation, CAFs or primary fibroblasts were injected into previous cancer sites, and the re-appearance and volume of radiated tumors were analyzed. As expected, compared to post-injection of primary fibroblasts or phosphate-buffered saline (PBS, control group), post-injection of CAFs significantly accelerated and enhanced the re-growth of radiated A375-xenografted cancers (Fig. 1B). Similar results were obtained using lung cancer A549-xenograft mouse model (Fig. S1).

Additionally, in a more clinically relevant setting, melanoma A375 cells and CAFs were first co-injected into the abdominal or forelimb armpits of nude mice, followed by a total of 30 Gy radiation in five fractions of 6 Gy once the tumor volume reached 150 mm^3. Half of the tumors in the CAF group were locally injected with the CAF inhibitor, Tranilast (Kissei Pharmaceuticals, Yoshino Matsumoto City Japan), 2 days before radiation (Ohshio et al., 2015; Ohshio et al., 2014). The observations on tumor re-appearance and volume were started 30 days after radiation therapy when tumors were undetectable by visual inspection. As shown in Fig. 1C, CAFs promoted an earlier and faster re-growth of A375 tumors than that of the control group (the A375 alone group), and the CAF inhibitor Tranilast significantly delayed and reduced A375 tumor re-growth post-radiotherapy when compared to the CAF group. Taken together, our findings demonstrated that CAFs promoted cancer recovery after radiation treatment.

3.2. CAF-derived Cytokine/Chemokines or Intermediate Metabolites Promoted Irradiated Cancer Cell Recovery

CAFs have been previously shown to produce a number of cytokines, which function to promote tumor development and progression (Boire et al., 2005; Ding et al., 2010). To explore the mechanisms underlying CAFs-induced cancer cell recovery from radiation-induced damage, cytokine antibody arrays were screened to identify potential cytokines and/or chemokines that may facilitate cancer cell recovery after radiation treatment (Fig. 2A). The top eight verified cytokines/chemokines that were significantly overexpressed in CAFs were then selected to individually test their effects on cancer cell survival post-radiation. As shown in Figs. 2B and S2A, three of these eight cytokines/chemokines, including IGF1, IGF2, and CXCL12, significantly increased irradiated (2 Gy) lung cancer A549 cancer cell survival. Similar results were obtained from melanoma A375 colony formation analyses (Fig. S2B), indicating that CAF promoted irradiated cancer cell recovery through production of particular cytokines/chemokines.

In addition to cytokines/chemokines, CAFs have also been reported to produce a larger amount of intermediate metabolites, such as lactate and ketone bodies, through metabolic reprogramming (Bonuccelli et al., 2010). To determine whether these intermediate metabolites generated by CAFs also played a role in irradiated cancer cell recovery, radiation-treated A549 cells were immediately cultured in medium containing lactate or β-hydroxybutyrate, two main metabolites secreted from CAFs. β-Hydroxybutyrate, but not lactate, enhanced the survival of A549 cells post-radiation (Fig. 2C), suggesting that specific metabolites produced by CAFs also contributed to the reduced radiation-induced cancer cell death.

To further confirm whether IGF1/2 and CXCL12 together reproduced the CAF effect on cancer cell recovery post-radiation, clonogenic assays were performed on A549 cells treated by the mixture of IGF1/2 and CXCL12. Compared to the control group, the combined treatment significantly promoted irradiated cancer cell recovery, and the colony numbers in the combined group were similar to that of the CAF-conditioned medium group ($p > 0.05$, Fig. 2D), suggesting IGF1/2 and CXCL12 were the factors promoting irradiated cancer cell recovery. To determine which factor was more responsible for irradiated cancer cell recovery, the clonogenic assays were first performed on lung cancer A549 cells cultured in CAF-conditioned medium with or without neutralizing antibody against IGF1, IGF2 or CXCL12. As shown in Fig. 2E, the IGF2 antibody significantly decreased cancer cell recovery post-radiation compared to the IGF1 or the CXCL12 antibody treated group, indicating that IGF2 was a major player in recovery of irradiated cancer cells.

To further confirm the effects of CAF-derived IGF2 on irradiated tumor relapse *in vivo*, we co-injected melanoma A375 cells into the abdominal armpits of nude mice with or without CAFs, that were infected by control viruses or viruses containing doxycycline-induced IGF2, IGF1 or CXCL12 shRNA. Once the tumor volume reached 150 mm^3, the mice were fed with drinking water containing 1 mg/ml of doxycycline/sucrose or sucrose alone for 1 week, followed by a total 30 of Gy radiation in five fractions of 6 Gy. As shown in Fig. 2F, the knockdown of IGF2 as well as IGF1/2/CXCL12 triple knockdown significantly delayed and reduced A375 tumor re-growth after radiotherapy compared to that of the control CAF group, suggesting that CAF-derived cytokines, particularly IGF2, promoted tumor cell recovery post-radiation.

3.3. Autophagy Suppression Reduced CAF-promoted Tumor Relapse Post-radiation

To further determine the molecular mechanisms by which growth factors and β-hydroxybutyrate reduced radiation-induced cancer cell death, we tested our hypothesis that these growth factors and metabolites were capable of inducing dormancy or autophagy, a special protective cellular status that is believed to ensure cancer cells have enough time for cellular damage repair (Farrow et al., 2014; Skvortsova et al., 2015; Yeh and Ramaswamy, 2015). Radiated A549 cells immediately cultured in CAF-conditioned medium or medium containing IGF2, EGF or β-hydroxybutyrate were analyzed for cell cycles progression 24 h after the culture period. As shown in Figs. 3A and S3A, CAF supernatant, IGF2, and β-hydroxybutyrate, but not EGF or lactate, significantly increased the subpopulation of cells at the G1/G0 phase compared to that of the control group, indicating that CAFs slowed down the cell cycle progression from G0/G1 to the S phase of A549 cells post-radiation. Moreover, this was coupled with enhanced phagosome formation, reflected by increased LC3 II protein levels (Fig. 3B) and LC3 foci (Fig. S3B). The greater number of cells at the G0/G1 phase correlated with a larger number of cells in autophagy. This finding was further confirmed by electron microscopy analysis (Fig. 3B). These observations demonstrated that CAFs induced autophagy in A549 tumor cells post-radiation through the secretion of specific cytokines or metabolites. In contrast, CAFs did not appear to induce A549 cells into dormancy status post-radiation, as the expression and/or phosphorylation of three cellular dormancy markers, Akt, p38 and Erk (Giancotti, 2013) were not decreased (Fig. S3C).

The mTOR is a major negative regulatory component of autophagy. Direct inhibitors of mTOR and pathways inactivating mTOR have been shown to induce autophagy (Farrow et al., 2014). To further determine whether CAF-induced post-radiation autophagy formation was able to promote tumor cell recovery, we analyzed the effects of rapamycin, a well-established mTOR inhibitor, on post-radiation survival of A549 cancer cells. As shown in Fig. 3C, Rapamycin increased A549 cancer cell survival post-radiation to the extent similar to the CAF-conditioned medium. When Atg5, a critical regulator of autophagy, was depleted, colony numbers decreased in all groups (Fig. S3D), and CAF-conditioned medium or the growth factor IGF1/2 could not further increased the colony numbers of A549 cancer cell any more (Fig. 3D), suggesting that CAF promoted irradiated tumor cell recovery through activating autophagy signaling.

The γ-H2Ax foci and comet tail moment, especially comet tail moment in the comet assay, are markers for double stranded DNA damage. The decrease in γ-H2Ax foci and comet tail moment within 3 h indicates that cells have enhanced capacity to repair damage for survival. To further confirm whether autophagy contributed to cancer recovery from radiation-induced DNA damage, the γ-H2Ax was detected and comet tail moment was measured at the indicated time points in A549 cells treated with CAF-conditioned medium, IGF2 or in the A549 cells depleted of Atg5. As shown in Figs. 3E, F, and S3e, both CAF and IGF2 remarkably reduced γ-H2Ax foci (3 ± 1 versus 9 ± 2) and comet tail moment ($10 \pm 2\%$ versus $36 \pm 4\%$) at 3 h post-radiation in A549 cells. However, when the critical autophagy regulator Atg5 was depleted, CAFs were not able to reduce γ-H2Ax foci and comet tail moment at the indicated time points, when compared to the control cell groups, which was consistent with the survival data in Fig. 3D. These observations suggested that CAF promoted DNA damage repair and tumor cell recovery post-radiation via the autophagy pathway.

3.4. CAF Inactivated mTOR Through Increasing PP2A Activity in Irradiated Cancer Cells

To determine how CAFs induced autophagy in irradiated cancer cells, the activity of mTOR, a major autophagy regulator, was first analyzed in lung cancer A549 cells treated post-radiation with or without IGF2, a main CAF-derived effector. As shown in Fig. 4A, IGF2 suppressed mTOR activation within 6 h of post-radiation; however, without radiation, IGF2 alone increased mTOR activity (Fig. S4A). This observation suggested that radiation altered the cellular response to IGF2 stimulation. To determine how the combined treatments of radiation and IGF2 decreased mTOR activity, the activation of mTOR upstream kinase AKT/ERK was analyzed in lung cancer A549 cells. As shown in Fig. S4B, IGF2 did not reduce the activity of AKT or ERK post-radiation, compared to the radiation alone treated cell groups. Therefore, we

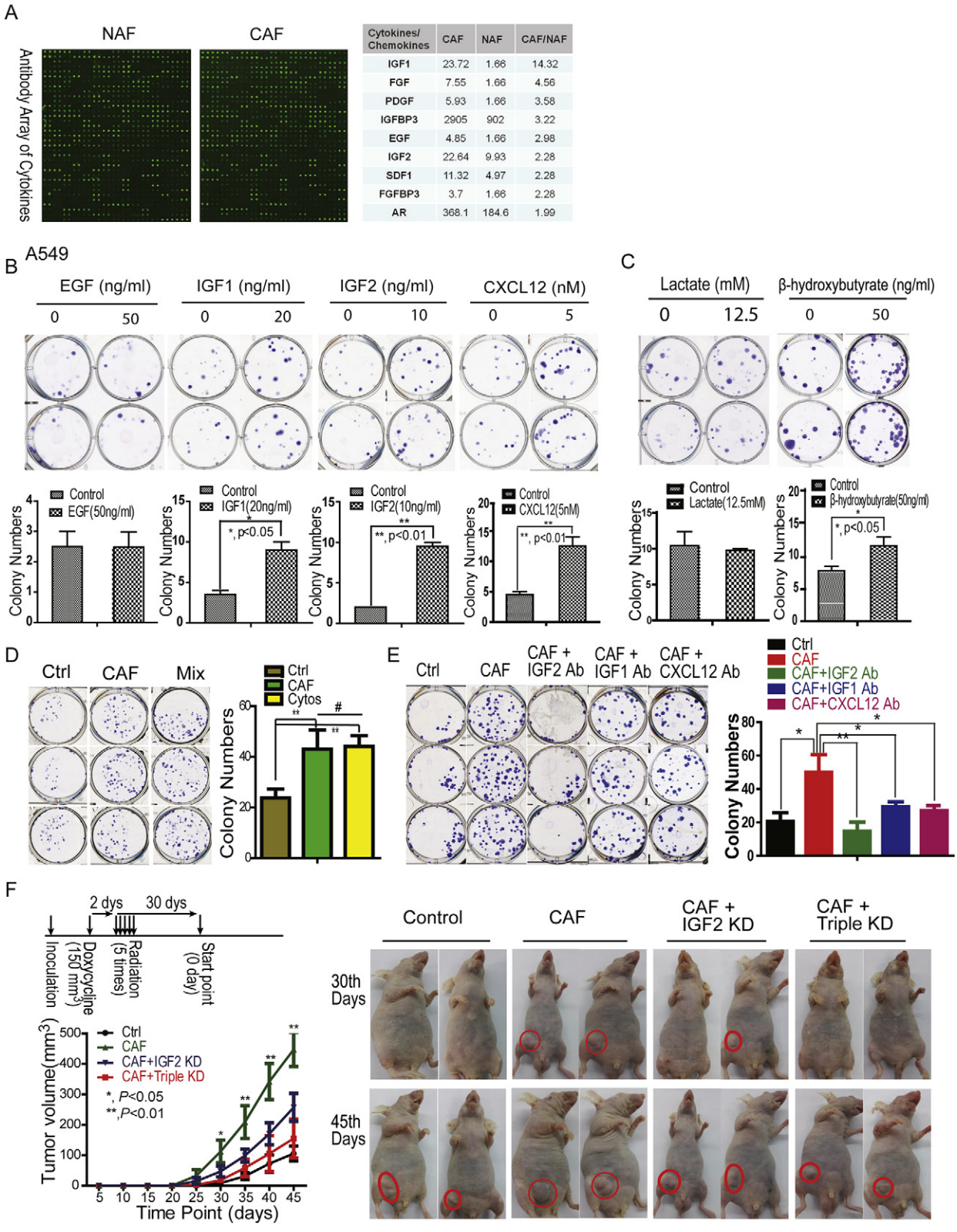

Cytokines/ Chemokines	CAF	NAF	CAF/NAF
IGF1	23.72	1.66	14.32
FGF	7.55	1.66	4.56
PDGF	5.93	1.66	3.58
IGFBP3	2905	902	3.22
EGF	4.85	1.66	2.98
IGF2	22.64	9.93	2.28
SDF1	11.32	4.97	2.28
FGFBP3	3.7	1.66	2.28
AR	368.1	184.6	1.99

Fig. 2. CAF-derived cytokines and metabolites promoted irradiated A549 cancer cell recovery. A. CAF-secreted cytokines/chemokines screening and verification. Cytokine antibody arrays were used and further verified by real time PCR. The selected cytokines/chemokines were presented in the right panel. B. & C. Effects of cytokines/chemokines or metabolites on cancer A549 cell recovery from radiation-induced cell death. The survival fraction of A549 cells were analyzed by clonogenic assays. D. The combination treatment of IGF1/2 and CXCL12 had a similar effect as CAF on cancer cell recovery postradiation. The final concentration of IGF1/2 and CXLC12 were 20 ng/mL, 10 ng/mL and 5 nM, respectively. E. IGF2 is a major growth factor for cancer cell recovery post-radiation. The final concentrations of antibodies were 1 μg/mL. F. IGF2 mediated CAF-promoted cancer recovery post-radiation. The experiment was performed as shown in the schematic drawing. Once the tumor volume reached 150 mm^3, the mice were given drinking water containing sucrose/doxycycline (1 mg/mL) or sucrose alone until five fractions of radiation, followed by a total of 50 Gy radiation in five fractions of 5 Gy each. IGF2 knockdown (KD) by doxycycline-inducible shRNAs. The triple KD: doxycycline-inducible IGF1, IGF2, and CXCL12 knockdown. The tumor volumes are presented as mean ± SD.

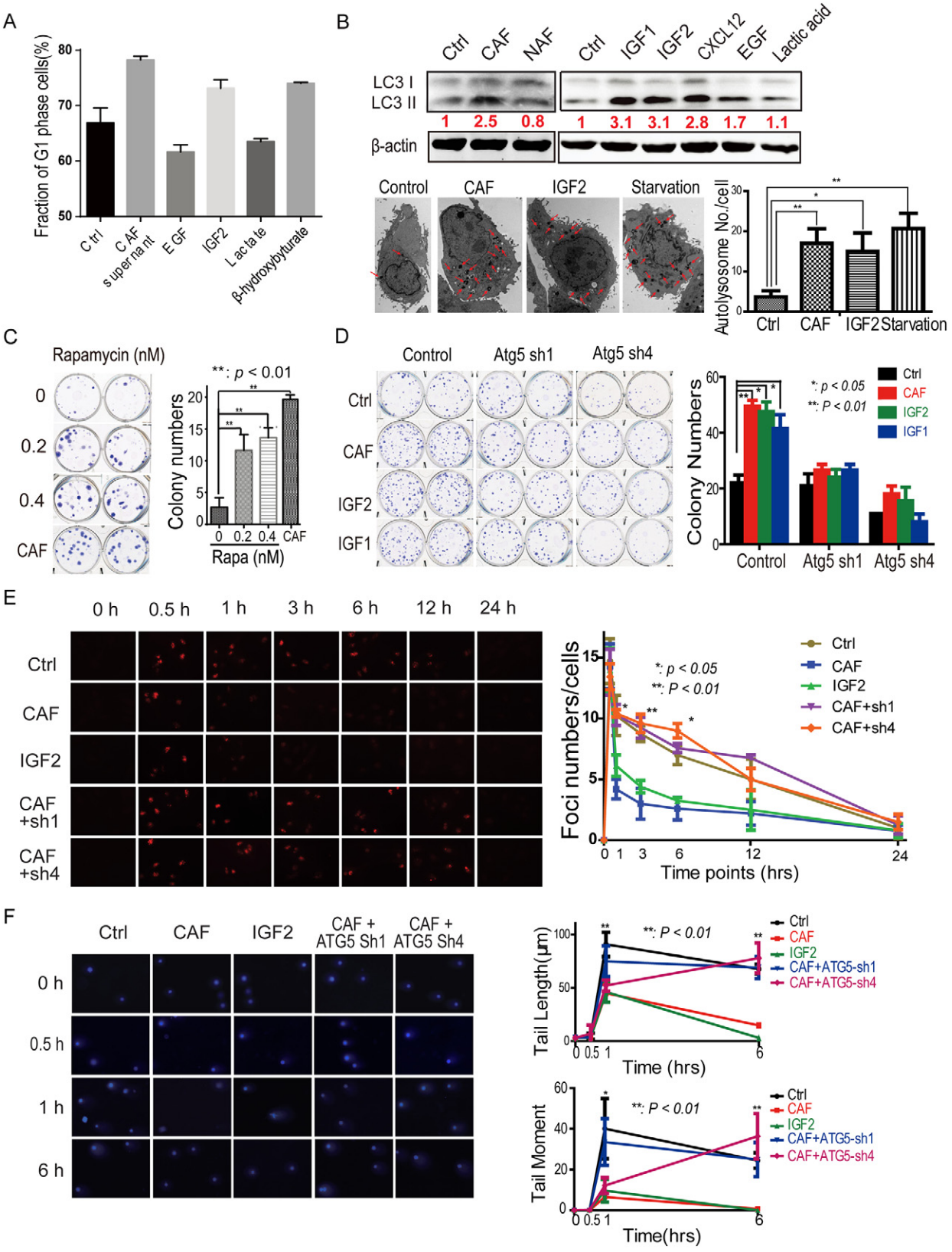

Fig. 3. Autophagy suppression reduced cancer-associated fibroblast (CAF)-promoted tumor relapse post-radiation. A. CAF induced autophagy formation in A549 cells post-radiation. The subpopulations of cells at the G1 phase of the cell cycle are presented by a histogram. The presented values are mean ± SD for triplicates. The protein levels of LC3 were detected in A549 cancer cells 6 h post-radiation. B. CAF induced autophagy formation in A549 cells through secreted cytokines and metabolites. The autophagy marker LC3 was detected by immunoblots and electron microscopy (EM) in A549 cells 6 h post-radiation. C. Rapamycin promoted A549 cell recovery from radiation-induced cell damage. The A549 cells were treated with 0.4 nm rapamycin. D. Atg5 knockdown decreased growth factors-increased A549 cells survival. E. and F. Atg5 knockdown impaired the DNA-damage repair in A549 cells treated with CAF-conditioned medium or IGF2. The γ-H2Ax foci were counted, the comet tail length was measured and the comet tail moment was analyzed as the formula (tail moment = (tail mean − head mean) × tail % DNA / 100) at the indicated time point, in one hundred cells randomly selected from each sample.

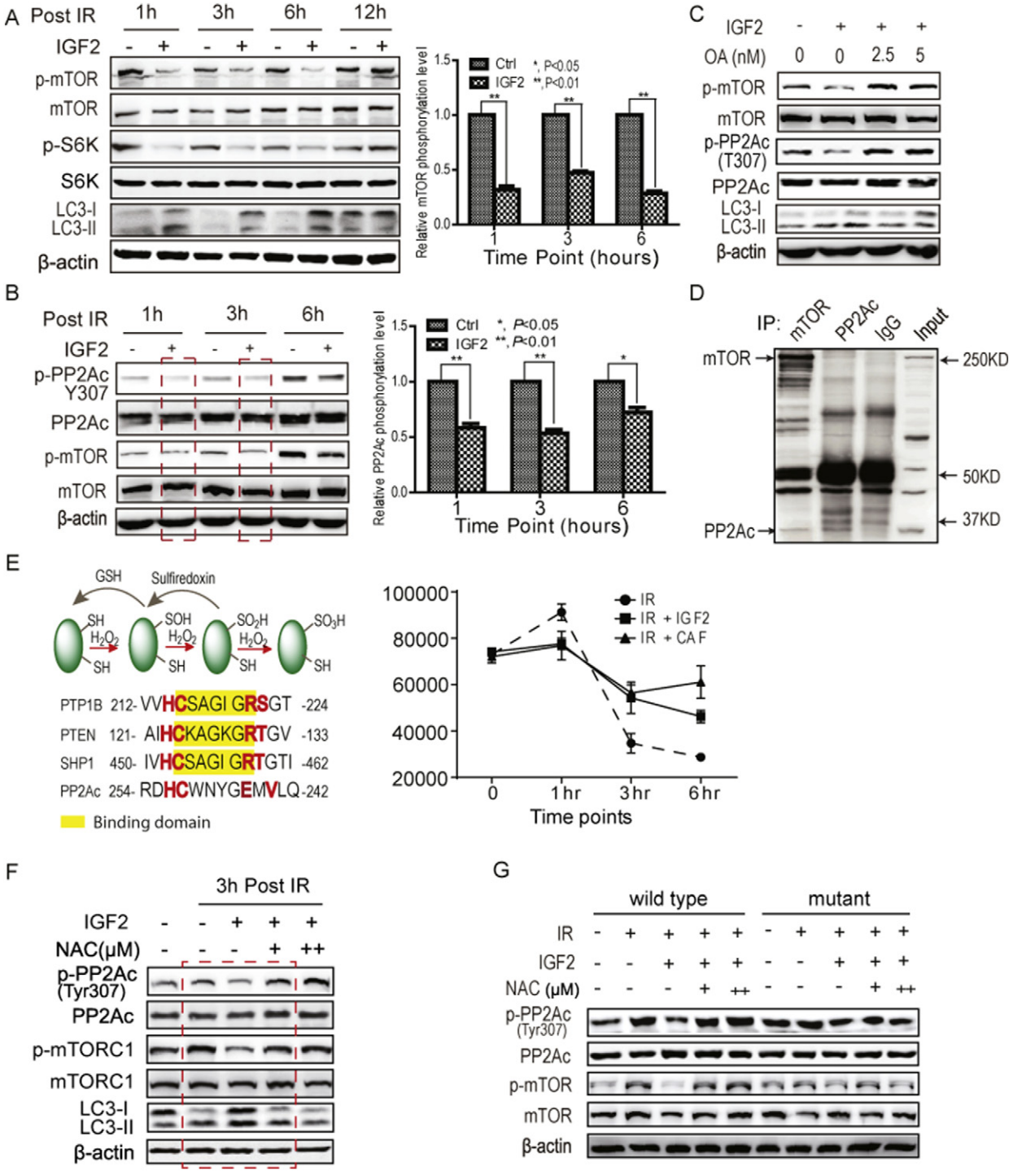

Fig. 4. CAFs suppressed mTOR activity through increasing PP2A activity in irradiated cancer cells. A. IGF2 suppressed mTOR activity in A549 cells post-radiation. A549 cells were treated with 2 Gy of radiation with or without 50 ng/mL of IGF2. B. IGF2 increased the activity of PP2A. PP2A activity was reflected by the dephosphorylation of T307 in A549 cells at 3 h post-radiation. The concentration of IGF2 was 50 ng/mL. C. The PP2A inhibitor, okadaic acid, restored IGF2-induced mTOR suppression post-radiation. D. The PP2Ac was associated with mTOR. The reciprocal co-immunoprecipitations were performed. E. IGF2 maintained the redox homeostasis in A549 cells post-radiation. The levels of reactive oxygen species (ROS) were analyzed by 2′,7′-dichlorodihydrofluorescein diacetate flow cytometry analyses of A549 cells post-radiation (2 Gy). F. The antioxidant *N*-acetylcysteine (NAC) abolished the IGF2-promoted PP2A activity. The concentration of NAC was 0.25 mM/mL (+) and 0.5 mM/mL (++), respectively. G. ROS regulated PP2A activity through the oxidation of Cys 251. The Cys 251 of PP2Ac was mutated to serine. The PP2A activity was analyzed at 3 h post-radiation. The concentrations of IGF2 and NAC were the same as described above.

speculated that an upstream phosphatase might dephosphorylate and inactivate mTOR.

Previous studies indicated that protein serine/threonine phosphatase PP2A might regulate autophagy (Apostolidis et al., 2016; Yang et al., 2016; Wong et al., 2015). Therefore, the activity of PP2A was first examined in A549 cells treated with or without IGF2 post-radiation. As shown in Fig. 4B, IGF2 increased the activity of PP2A, which is reflected by the Tyr307 dephosphorylation of PP2Ac and closely correlated with mTOR inactivation. Moreover, the PP2A inhibitor okadaic acid (OA) abolished IGF2 suppression of mTOR activity and increased mTOR activation (Fig. 4C).

To determine whether the phosphatase PP2A directly regulates mTORC1 activity, the physical association of PP2A with mTOR was examined by reciprocal immunoprecipitation from A549 cells. As shown in Fig. 4D, the mTOR was co-immunoprecipitated by the specific antibody against PP2Ac (PP2A catalytic subunit), and vice versa, suggesting that PP2A formed a complex with mTOR. Taken together, these observations suggested that CAF promoted PP2A activation post-radiation, which, in turn, suppressed mTOR activity.

Reactive oxygen species (ROS) react with low pKa protein thiols, such as those on cysteine to form sulfenic acid (R-SOH) (Manevich et al., 2004) and ROS is co-regulated by growth factor activation of NADPH-dependent oxidases (NOXs) (Samarakoon et al., 2013; Trachootham et al., 2008; Truong and Carroll, 2012). Protein tyrosine phosphatases (PTPs) can be inactivated by the ROS-catalyzed sulfenylation at the conserved motif of $HC(X)_5RS/T$ (Fig. 4E). Through protein sequence analysis, we showed that the motif of $HC(X)_4EXV$ in PP2Ac was similar to the motif of $HC(X)_5RS/T$ in PTPs. To determine whether PP2A activity was regulated by ROS, the levels of ROS post-radiation were analyzed by flow cytometry after dichlorodihydrofluorescein (DCFDA) staining. As shown in Fig. 4E, both CAF-conditioned medium and IGF2 treatment prevented cellular ROS levels from decreasing and maintained a relatively high level of ROS, compared to the radiation alone group. To identify whether this increase in ROS modulates the PP2A activity, lung cancer A549 cells were treated with IGF2 and the antioxidant *N*-acetylcysteine (NAC) immediately after radiation. As shown in Fig. 4F, NAC abolished the IGF2-increased PP2A activity and inhibited autophagy, suggesting that CAFs promote PP2A activation post-radiation through increased ROS.

To further determine whether Cys251 of PP2Ac regulates the PP2A activity, the Cys251 was replaced with serine and the activity of PP2Ac was analyzed in 239T cells overexpressing wild type or mutant PP2Ac. As shown in Fig. 4G, IGF2 treatment increased the activity of PP2A post-radiation while NAC impaired this activation. However, the C251S mutation of PP2Ac abolished this enhancement, suggesting Cys251 was critical for PP2A activity, and that the oxidation of Cys251 enhanced the PP2A activity. These observations indicated that IGF2 enhanced PP2A activity post-radiation through the increase in ROS levels, and PP2A, in turn, suppressed mTOR activity, increased autophagy.

3.5. Autophagy Suppression Reduced CAF-promoted Tumor Relapse Post-radiation

The above data demonstrated that CAF promoted irradiated cancer cell recovery through mTOR-mediated autophagy, suggesting that targeting the autophagy pathway is a promising strategy for radiosensitization. To determine whether autophagy inhibition interrupted CAF-promoted cancer recurrence post-radiation, we co-injected A549 cancer cells with or without CAF into the abdominal or forelimb armpits of nude mice. As shown in Fig. 5A, the IGF2 neutralizing antibody or the autophagy inhibitor 3-MA was locally injected into tumors in the CAF group when tumor volumes reached 150 mm^3, followed by a total of 30 Gy radiotherapy in five fractions of 6 Gy. Compared to the control group, CAFs significantly accelerated and enhanced the re-growth of the xenografted tumors post-radiation; both IGF2 neutralizing antibody and autophagy inhibitor 3-MA attenuated the CAF-enhanced reappearance and re-growth of A549-xenografted tumors (Fig. 5B, C). Fluorescence staining of the sections of xenografted tumors showed that CAFs promoted cancer cell autophagy and the down-regulation of IGF2 suppressed autophagy formation (Fig. 5D). This observation further confirmed that CAFs promoted cancer cell recovery post-radiation through IGF2 and that autophagy mediated this enhancement, suggesting that CAF-secreted growth factors or mTOR may be potential targets to improve the efficacy of radiotherapy.

3.6. SBRT Therapy Which Leads to Less Damage to CAFs Might Promote Survival and Relapse of Tumor Patients

Based on our previous findings (Zhang et al., 2015) and the principles of magnetic resonance imaging (MRI) or computed tomography (CT) imaging, MRI or CT scans might fail to reveal the CAFs in the outer tumor regions (Fig. S6A), and untargeted or less damaged CAFs in this region could potentiate tumor relapse. The current advanced technology, an image-guided stereotactic body radiation therapy (SBRT), aims to precisely deliver radiation doses to cancer regions and reduce the damage to normal tissues, compared to the conventional external beam radiotherapy (EBRT). We hypothesized that SBRT that leads to less damage or is untargeted to CAFs in the outer tumor region would be less effective than the conventional external beam radiotherapy in terms of the recurrence and survival of cancer patients.

To test this hypothesis, we performed a retrospective study to analyze the recurrence time and survival of lung cancer patients with SBRT. The tumor patients in this study were at early stage and were unresectable. Our data showed that cancer recurrence, including local and remote, in patients with conventional EBRT treatment was less frequent than in patients with SBRT. The average recurrence interval for the two groups was 36 months versus 28 months, respectively (Fig. 6A). The survival time of patients with EBRT was also longer than for patients with SBRT, 56 months versus 39 months, respectively (the median, Fig. 6B). Moreover, a similar study on hepatocellular carcinoma patients showed consistent results, indicating that the EBRT had better therapeutic effects than SBRT (Fig. S6B, C), further suggesting that the SBRT that fails to damage the surrounding CAFs might less effective than the EBRT in terms of recurrence and survival of cancer patients, further supporting the hypothesis that CAFs promote cancer cell recovery and tumor relapse post-radiation.

4. Discussion

Radiation therapy, one of three conventional treatments for cancer patients, kills cancer cells by damaging their DNA directly or creating charged particles (free radicals) (Lawrence et al., 2008). Recent technical improvements, such as SBRT or stereotactic radiosurgery, provide real-time imaging of tumors for precise dose delivery (Bernstein et al., 2016). This technology helps to compensate for normal movement of the internal organs due to breathing and for changes occurring in cancer size during treatment, thereby reducing unnecessary doses to normal tissues (Gabriely et al., 2008). However, tumor relapse post-radiotherapy is still a challenge to clinical oncologists.

In this study, we showed that CAFs increased irradiated tumor cell recovery through enhancing autophagy in tumor cells. In addition, our data have also demonstrated that preexisting CAFs promote tumor cell resistance to radiation *in vitro* and *in vivo* through increasing the subpopulation of cancer initiating cells before radiation (Fig. S7), which were consistent with previous studies (Bao et al., 2006; Phillips et al., 2006). These observations indicate that CAF-induced stem-like property of cancer cells is a long term effect whereas CAF-promoted irradiated tumor cell recovery is an instant response. Taken together, CAFs contribute to tumor cell survival post-radiation not only before treatment, but also post-radiation, both are important for cancer survival post-radiation, although their underlying mechanisms are distinct.

Moreover, our results further showed that CAFs, as the second largest cell population in tumors, are not only tangled with tumor cells, but also exist in tumor region without tumor cells, which was much wider than previously expected. Currently, the tumor is detected in clinics by MRI or CT, which could not be capable to reveal the CAF region in the outer tumor region. Therefore, these untargeted or less damaged CAFs would lead to increasing cancer relapse and poor prognosis in image-guided radiation therapy, and a new method which can reveal the whole region of tumor is indispensable to improving the efficacy

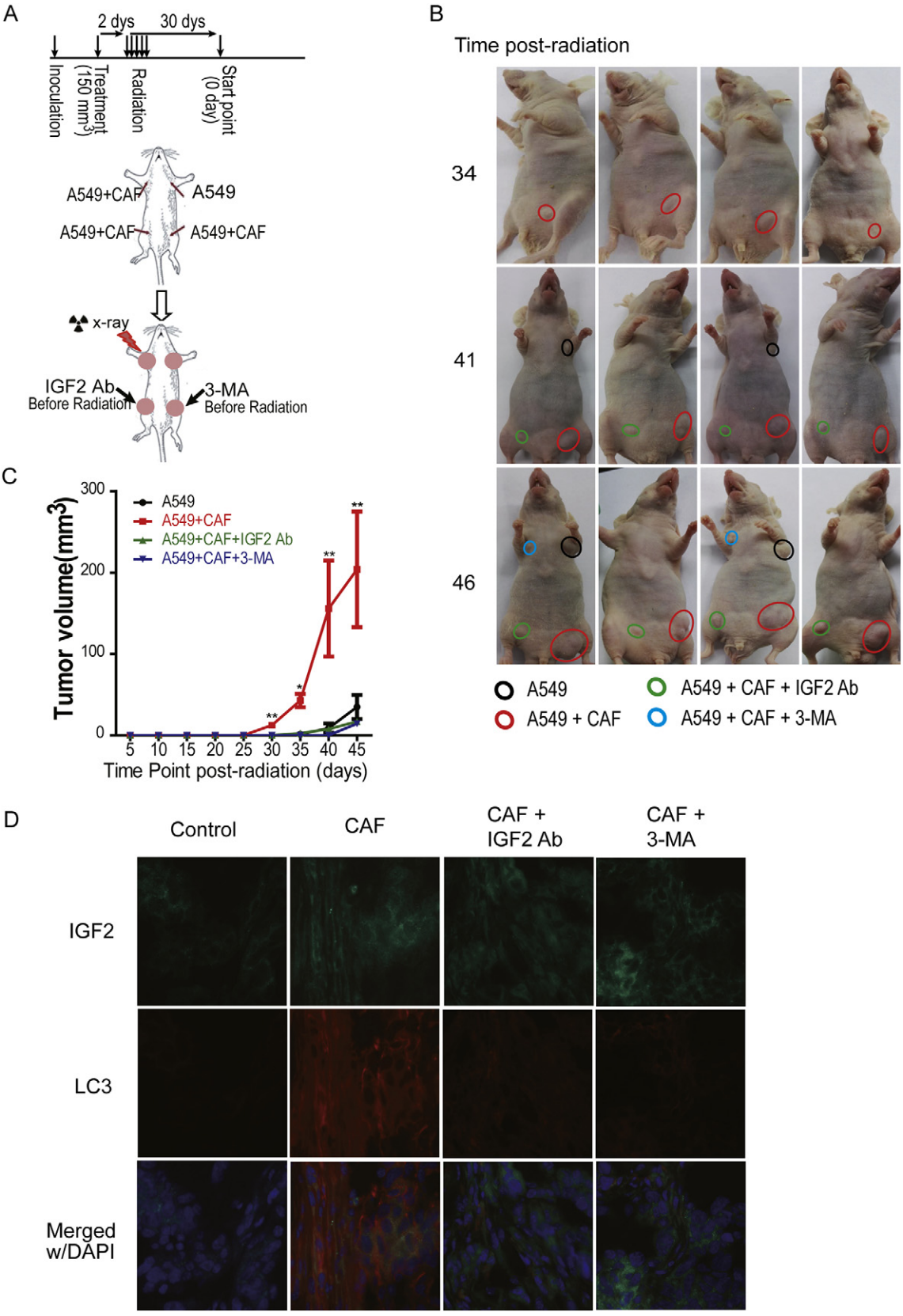

Fig. 5. Autophagy suppression reduced CAF-promoted tumor relapse post-radiation *in vivo*. A. The schematic drawing of the animal experiment. B. The representative tumors at the indicated time points (10 tumors in each group). The mice were received radiation at a total of 30 Gy in 5 fractions. C. The effect of autophagy inhibitor 3-methyladenine (3-MA, 5 mM) and IGF2 neutralizing antibody (1 μg/ml) on tumor recurrence. The tumor sizes were measured every 5 days, and the tumor volumes were calculated using the formula described above. D. The detection of IGF2 and LC3 expression in xenografted tumors. The magnification is 10×.

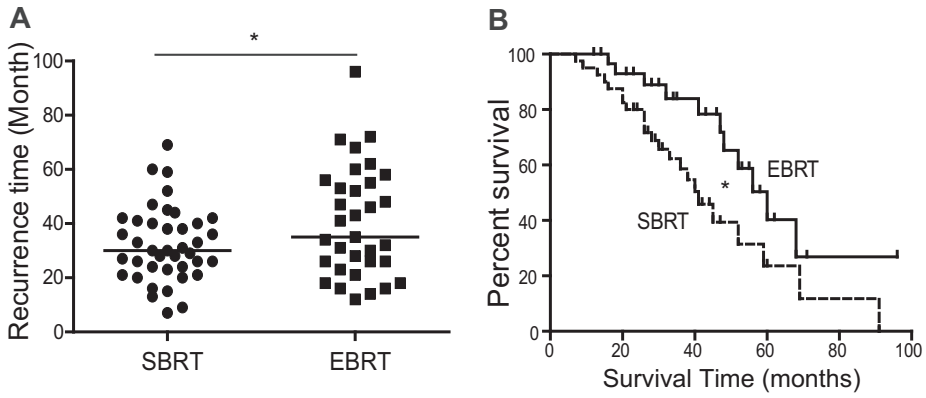

Fig. 6. Stereotactic body radiation therapy was less damaging to CAFs and might promote the survival and relapse of tumor patients. A. The SBRT treatment (40 cases) accelerated the recurrence of patients with lung cancer (*, $p < 0.05$), compared to the patients with the EBRT treatment (33 cases). The total radiation dose was 65 ± 5 Gy. B. The SBRT treatment shortened the survival of patients with lung cancer (*, $p < 0.05$), compared to the patients with the external beam radiotherapy (EBRT) treatment. The recurrent free survival was analyzed by the Kaplan-Meier method.

of radiotherapy on tumor patients, especially to the image-guided radiation therapy or surgical therapy.

Autophagy, first discovered in nutrition-deprived cells, is a double-edged sword to cell survival, and the degree of autophagy is critical to its effect. Low levels of autophagy and cell dormancy may be protective response to prevent cells from dying (Morgan-Bathke et al., 2014; Smith and Freeman, 2014; Palumbo and Comincini, 2013; Apel et al., 2008). Autophagy was also induced by other stresses such as low dose of radiation (Smith and Freeman, 2014; Liang et al., 2013; Paglin et al., 2001). In this study, we have demonstrated that CAFs promoted autophagy, but not dormancy, in irradiated cancer cells, and that autophagy increased cancer cell recovery from radiation-induced cell damage. IGF2was one of the CAF-secreted factors that mainly mediated CAF suppression of mTOR activity and induced autophagy formation in irradiated cancer cells, this effect was distinct from the effect of IGF2 without radiation.

The mTOR is a master regulator of autophagy and is activated by its upstream kinases and by phosphatases such as PP2A. Starvation increased phosphatase PP2A activity to dephosphorylate ULK1, an mTORC1 substrate whose dephosphorylation was required for autophagy induction (Wong et al., 2015). Moreover, the activity of PP2A was also required in pancreatic ductal adenocarcinoma cells for sustained anchorage-independent growth, which depended on high basal autophagy. In addition, in response to amino acid deprivation, the phosphatase PP2A regulated autophagy through dephosphorylating MAP4K3, an upstream kinase of mTOR (Yan et al., 2010).

Protein tyrosine phosphatases (PTPs) are inactivated by ROS-catalyzed sulfenylation at the conserved motif HC(X)5RS/T, since this motif overlaps with the substrate binding site of PTPs and this sulfenylation interrupts the binding with substrate (Fig. 4E). PP2Ac has a motif of $HC(X)_4EXV$ that is similar to the motif of $HC(X)_5RS/T$ in PTPs, of which the cysteine residue can be sulfenylated by increased ROS. However, unlike the PTPs, sulfenylation increases PP2Ac activity. We have shown that IGF2 maintained ROS levels in cancer cells post-radiation, and resulted in a relatively higher ROS levels than that of the only irradiated control cells. These observations suggested that the mechanism underlying radiation-induced autophagy different from the IGF2-promoted autophagy post-radiation.

In summary, we have shown that CAFs are critical in promoting cancer cell recovery from radiation-induced damage and re-growth. Our results further showed that CAFs, as the second largest cell population in tumors, distribute around tumors in a much wider region than previously expected. These CAFs in the outer tumors allows easy escape of CAFs, as demonstrated in image-guided radiation therapy, leading to increasing cancer relapse and poor prognosis. Our findings suggest that the targeting autophagy pathway in tumor cells is a promising therapeutic strategy for reducing cancer relapse and improving radiation efficiency.

Conflict of Interest Disclosure

All authors state there are no conflicts of interest to disclose.

Author Contribution Statement

Y.W., G.G. and J.W. performed most of the experiments; B.W. and D.Z. performed MRI and MRS scans; Y.C., Y.X. and X.W. performed some of the experiments; H.H., M.Y. and J.Z. participated in the clinical study and analyzed the clinical data; X.L. provided reagents and revised the paper; J. M. designed the project and wrote the article; all authors reviewed the manuscript.

Acknowledgements

We are grateful to Dr. Shimin Zhao (Fudan University), Qiang Liu (Dalian Medical University), and Dr. Jinke Cheng, Dr. Zhaoyuan Hou and Dr. Xuemei Tong (Shanghai Jiao Tong University School of Medicine) for valuable discussions. This study was supported by grants from the National Program on Key Basic Research Project (973 Program) (2012CB910102), the Shanghai Municipal Science and Technology Commission (11DZ2260200), and the National Science Foundation of China (81372194, 81572300) to Dr. Mi.

Appendix A. Supplementary Data

Supplemental figures are available online. Supplementary data associated with this article can be found in the online version, at http://dx.doi.org/10.1016/j.ebiom.2017.02.019.

References

Apel, A., Herr, I., Schwarz, H., Rodemann, H.P., Mayer, A., 2008. Blocked autophagy sensitizes resistant carcinoma cells to radiation therapy. Cancer Res. 68, 1485–1494.
Apostolidis, S.A., Rodriguez-Rodriguez, N., Suarez-Fueyo, A., Dioufa, N., Ozcan, E., Crispin, J.C., Tsokos, M.G., Tsokos, G.C., 2016. Phosphatase PP2A is requisite for the function of regulatory T cells. Nat. Immunol. 17, 556–564.
Bao, S., Wu, Q., McLendon, R.E., Hao, Y., Shi, Q., Hjelmeland, A.B., Dewhirst, M.W., Bigner, D.D., Rich, J.N., 2006. Glioma stem cells promote radioresistance by preferential activation of the DNA damage response. Nature 444, 756–760.
Bao, B., Ahmad, A., Azmi, A.S., Ali, S., Sarkar, F.H., 2013. Overview of cancer stem cells (CSCs) and mechanisms of their regulation: implications for cancer therapy. Curr. Protoc. Pharmacol. 14 Unit–14.25.
Bernstein, M.B., Krishnan, S., Hodge, J.W., Chang, J.Y., 2016. Immunotherapy and stereotactic ablative radiotherapy (ISABR): a curative approach? Nat. Rev. Clin. Oncol. 13, 516–524.
Bhowmick, N.A., Neilson, E.G., Moses, H.L., 2004. Stromal fibroblasts in cancer initiation and progression. Nature 432, 332–337.
Boire, A., Covic, L., Agarwal, A., Jacques, S., Sherifi, S., Kuliopulos, A., 2005. PAR1 is a matrix metalloprotease-1 receptor that promotes invasion and tumorigenesis of breast cancer cells. Cell 120, 303–313.

Bonuccelli, G., Tsirigos, A., Whitaker-Menezes, D., Pavlides, S., Pestell, R.G., Chiavarina, B., Frank, P.G., Flomenberg, N., Howell, A., Martinez-Outschoorn, U.E., et al., 2010. Ketones and lactate "fuel" tumor growth and metastasis: evidence that epithelial cancer cells use oxidative mitochondrial metabolism. Cell Cycle 9, 3506–3514.

Burns, J.L., Hassan, A.B., 2001. Cell survival and proliferation are modified by insulin-like growth factor 2 between days 9 and 10 of mouse gestation. Development 128, 3819–3830.

Capparelli, C., Guido, C., Whitaker-Menezes, D., Bonuccelli, G., Balliet, R., Pestell, T.G., Goldberg, A.F., Pestell, R.G., Howell, A., Sneddon, S., et al., 2012. Autophagy and senescence in cancer-associated fibroblasts metabolically supports tumor growth and metastasis via glycolysis and ketone production. Cell Cycle 11, 2285–2302.

Carmeliet, P., Jain, R.K., 2000. Angiogenesis in cancer and other diseases. Nature 407, 249–257.

Chaudhury, A., Hussey, G.S., Ray, P.S., Jin, G., Fox, P.L., Howe, P.H., 2010. TGF-beta-mediated phosphorylation of hnRNP E1 induces EMT via transcript-selective translational induction of Dab2 and ILEI. Nat. Cell Biol. 12, 286–293.

Chen, W.J., Ho, C.C., Chang, Y.L., Chen, H.Y., Lin, C.A., Ling, T.Y., Yu, S.L., Yuan, S.S., Chen, Y.J., Lin, C.Y., et al., 2014. Cancer-associated fibroblasts regulate the plasticity of lung cancer stemness via paracrine signalling. Nat. Commun. 5, 3472.

Chu, T.Y., Yang, J.T., Huang, T.H., Liu, H.W., 2014. Crosstalk with cancer-associated fibroblasts increases the growth and radiation survival of cervical cancer cells. Radiat. Res. 181, 540–547.

Dimanche-Boitrel, M.T., Vakaet Jr., L., Pujuguet, P., Chauffert, B., Martin, M.S., Hammann, A., Van Roy, F., Mareel, M., Martin, F., 1994. In vivo and in vitro invasiveness of a rat colon-cancer cell line maintaining E-cadherin expression: an enhancing role of tumor-associated myofibroblasts. Int. J. Cancer 56, 512–521.

Ding, Y., Kim, J.K., Kim, S.I., Na, H.J., Jun, S.Y., Lee, S.J., Choi, M.E., 2010. TGF-{beta}1 protects against mesangial cell apoptosis via induction of autophagy. J. Biol. Chem. 285, 37909–37919.

Farrow, J.M., Yang, J.C., Evans, C.P., 2014. Autophagy as a modulator and target in prostate cancer. Nat. Rev. Urol. 11, 508–516.

Fiaschi, T., Marini, A., Giannoni, E., Taddei, M.L., Gandellini, P., De Donatis, A., Lanciotti, M., Serni, S., Cirri, P., Chiarugi, P., 2012. Reciprocal metabolic reprogramming through lactate shuttle coordinately influences tumor-stroma interplay. Cancer Res. 72, 5130–5140.

Frank, N.Y., Schatton, T., Frank, M.H., 2010. The therapeutic promise of the cancer stem cell concept. J. Clin. Invest. 120, 41–50.

Franken, N.A., Rodermond, H.M., Stap, J., Haveman, J., van Bree, C., 2006. Clonogenic assay of cells in vitro. Nat. Protoc. 1, 2315–2319.

Gabriely, G., Wurdinger, T., Kesari, S., Esau, C.C., Burchard, J., Linsley, P.S., Krichevsky, A.M., 2008. MicroRNA 21 promotes glioma invasion by targeting matrix metalloproteinase regulators. Mol. Cell. Biol. 28, 5369–5380.

Giancotti, F.G., 2013. Mechanisms governing metastatic dormancy and reactivation. Cell 155, 750–764.

Grum-Schwensen, B., Klingelhofer, J., Berg, C.H., El-Naaman, C., Grigorian, M., Lukanidin, E., Ambartsumian, N., 2005. Suppression of tumor development and metastasis formation in mice lacking the S100A4(mts1) gene. Cancer Res. 65, 3772–3780.

Klaude, M., Eriksson, S., Nygren, J., Ahnstrom, G., 1996. The comet assay: mechanisms and technical considerations. Mutat. Res. 363, 89–96.

Kolch, W., Martiny-Baron, G., Kieser, A., Marme, D., 1995. Regulation of the expression of the VEGF/VPS and its receptors: role in tumor angiogenesis. Breast Cancer Res. Treat. 36, 139–155.

Lawrence, Y.R., Werner-Wasik, M., Dicker, A.P., 2008. Biologically conformal treatment: biomarkers and functional imaging in radiation oncology. Future Oncol. 4, 689–704.

Lengauer, C., Kinzler, K.W., Vogelstein, B., 1998. Genetic instabilities in human cancers. Nature 396, 643–649.

Liang, N., Jia, L., Liu, Y., Liang, B., Kong, D., Yan, M., Ma, S., Liu, X., 2013. ATM pathway is essential for ionizing radiation-induced autophagy. Cell. Signal. 25, 2530–2539.

Lochter, A., Galosy, S., Muschler, J., Freedman, N., Werb, Z., Bissell, M.J., 1997. Matrix metalloproteinase stromelysin-1 triggers a cascade of molecular alterations that leads to stable epithelial-to-mesenchymal conversion and a premalignant phenotype in mammary epithelial cells. J. Cell Biol. 139, 1861–1872.

Manevich, Y., Feinstein, S.I., Fisher, A.B., 2004. Activation of the antioxidant enzyme 1-CYS peroxiredoxin requires glutathionylation mediated by heterodimerization with pi GST. Proc. Natl. Acad. Sci. U. S. A. 101, 3780–3785.

Morgan-Bathke, M., Hill, G.A., Harris, Z.I., Lin, H.H., Chibly, A.M., Klein, R.R., Burd, R., Ann, D.K., Limesand, K.H., 2014. Autophagy correlates with maintenance of salivary gland function following radiation. Sci. Report. 4, 5206.

Ohshio, Y., Hanaoka, J., Kontani, K., Teramoto, K., 2014. Tranilast inhibits the function of cancer-associated fibroblasts responsible for the induction of immune suppressor cell types. Scand. J. Immunol. 80, 408–416.

Ohshio, Y., Teramoto, K., Hanaoka, J., Tezuka, N., Itoh, Y., Asai, T., Daigo, Y., Ogasawara, K., 2015. Cancer-associated fibroblast-targeted strategy enhances antitumor immune responses in dendritic cell-based vaccine. Cancer Sci. 106, 134–142.

Olaso, E., Santisteban, A., Bidaurrazaga, J., Gressner, A.M., Rosenbaum, J., Vidal-Vanaclocha, F., 1997. Tumor-dependent activation of rodent hepatic stellate cells during experimental melanoma metastasis. Hepatology 26, 634–642.

Olumi, A.F., Grossfeld, G.D., Hayward, S.W., Carroll, P.R., Tlsty, T.D., Cunha, G.R., 1999. Carcinoma-associated fibroblasts direct tumor progression of initiated human prostatic epithelium. Cancer Res. 59, 5002–5011.

Orimo, A., Gupta, P.B., Sgroi, D.C., Arenzana-Seisdedos, F., Delaunay, T., Naeem, R., Carey, V.J., Richardson, A.L., Weinberg, R.A., 2005. Stromal fibroblasts present in invasive human breast carcinomas promote tumor growth and angiogenesis through elevated SDF-1/CXCL12 secretion. Cell 121, 335–348.

Osuka, S., Sampetrean, O., Shimizu, T., Saga, I., Onishi, N., Sugihara, E., Okubo, J., Fujita, S., Takano, S., Matsumura, A., et al., 2013. IGF1 receptor signaling regulates adaptive radioprotection in glioma stem cells. Stem Cells 31, 627–640.

Paglin, S., Hollister, T., Delohery, T., Hackett, N., McMahill, M., Sphicas, E., Domingo, D., Yahalom, J., 2001. A novel response of cancer cells to radiation involves autophagy and formation of acidic vesicles. Cancer Res. 61, 439–444.

Palumbo, S., Comincini, S., 2013. Autophagy and ionizing radiation in tumors: the "survive or not survive" dilemma. J. Cell. Physiol. 228, 1–8.

Phillips, T.M., McBride, W.H., Pajonk, F., 2006. The response of CD24(−/low)/CD44+ breast cancer-initiating cells to radiation. J. Natl. Cancer Inst. 98, 1777–1785.

Ronnov-Jessen, L., Petersen, O.W., Bissell, M.J., 1996. Cellular changes involved in conversion of normal to malignant breast: importance of the stromal reaction. Physiol. Rev. 76, 69–125.

Saharinen, P., Eklund, L., Pulkki, K., Bono, P., Alitalo, K., 2011. VEGF and angiopoietin signaling in tumor angiogenesis and metastasis. Trends Mol. Med. 17, 347–362.

Samarakoon, R., Overstreet, J.M., Higgins, P.J., 2013. TGF-beta signaling in tissue fibrosis: redox controls, target genes and therapeutic opportunities. Cell. Signal. 25, 264–268.

Sandler, A.B., Johnson, D.H., Herbst, R.S., 2004. Anti-vascular endothelial growth factor monoclonals in non-small cell lung cancer. Clin. Cancer Res. 10, 4258s–4262s.

Singh, N.P., McCoy, M.T., Tice, R.R., Schneider, E.L., 1988. A simple technique for quantitation of low levels of DNA damage in individual cells. Exp. Cell Res. 175, 184–191.

Skvortsova, I., Debbage, P., Kumar, V., Skvortsov, S., 2015. Radiation resistance: cancer stem cells (CSCs) and their enigmatic pro-survival signaling. Semin. Cancer Biol. 35, 39–44.

Smith, C.A., Freeman, M.L., 2014. Oncology scan—autophagy and the radiation response. Int. J. Radiat. Oncol. Biol. Phys. 90, 7–10.

Tlsty, T.D., 2001. Stromal cells can contribute oncogenic signals. Semin. Cancer Biol. 11, 97–104.

Trachootham, D., Lu, W., Ogasawara, M.A., Nilsa, R.D., Huang, P., 2008. Redox regulation of cell survival. Antioxid. Redox Signal. 10, 1343–1374.

Truong, T.H., Carroll, K.S., 2012. Redox regulation of epidermal growth factor receptor signaling through cysteine oxidation. Biochemistry 51, 9954–9965.

Visvader, J.E., Lindeman, G.J., 2008. Cancer stem cells in solid tumours: accumulating evidence and unresolved questions. Nat. Rev. Cancer 8, 755–768.

Wong, P.M., Feng, Y., Wang, J., Shi, R., Jiang, X., 2015. Regulation of autophagy by coordinated action of mTORC1 and protein phosphatase 2A. Nat. Commun. 6, 8048.

Xing, Y., Zhao, S., Zhou, B.P., Mi, J., 2015. Metabolic reprogramming of the tumour microenvironment. FEBS J. 282, 3892–3898.

Yan, L., Mieulet, V., Burgess, D., Findlay, G.M., Sully, K., Procter, J., Goris, J., Janssens, V., Morrice, N.A., Lamb, R.F., 2010. PP2A T61 epsilon is an inhibitor of MAP4K3 in nutrient signaling to mTOR. Mol. Cell 37, 633–642.

Yang, Z.J., Wechsler-Reya, R.J., 2007. Hit 'em where they live: targeting the cancer stem cell niche. Cancer Cell 11, 3–5.

Yang, X., Zhang, Y., Liu, H., Lin, Z., 2016. Cancerous inhibitor of PP2A silencing inhibits proliferation and promotes apoptosis in human multiple myeloma cells. Biomed. Res. Int. 2016, 6864135.

Yeh, A.C., Ramaswamy, S., 2015. Mechanisms of cancer cell dormancy-another hallmark of cancer? Cancer Res. 75, 5014–5022.

Zhang, D., Wang, Y., Shi, Z., Liu, J., Sun, P., Hou, X., Zhang, J., Zhao, S., Zhou, P.B., Mi, J., 2015. Metabolic reprogramming of cancer-associated fibroblast by IDH3. Cell Rep. 10, 14.